Absolute, On-Line Monitoring of Molar Mass during Polymerization Reactions

Fabio Herbst Florenzano, Roland Strelitzki, and Wayne F. Reed*

Physics Department, Tulane University, New Orleans, Louisiana 70118

Received June 2, 1998; Revised Manuscript Received August 4, 1998

ABSTRACT: To perform on-line monitoring of the absolute weight-averaged mass, M_w, of the polymers produced in a polymerization reaction, refractometer (RI), ultraviolet absorbance (UV), and time-dependent static light scattering (TDSLS) detectors were placed in series, and a diluted stream of reactant solution was made to flow through them. The technique allows rapid determination of time-dependent reaction "signatures" and end-product masses. Hence the effects of changing reaction conditions such as reactant concentrations, temperature, and initiators can be quickly assessed. Such a technique is expected to be of wide utility in characterizing polymerization reactions, both on the laboratory scale, where new polymers are synthesized and conditions optimized, as well as on the industrial scale, where on-line quality control can be performed. For stepwise reactions, the RI and TDSLS detectors are sufficient for determination of M_w, whereas for free radical reactions, the polymer concentration must be measured in order to obtain the traditionally defined M_w (i.e. without monomer taken into consideration). The latter was achieved for poly(vinyl pyrrolidinone) polymerization by measuring the monomer concentration with the UV detector. As a further measure of characterization, a single capillary viscometer was also placed in series with the other instruments. This allowed the reduced viscosity to be monitored simultaneously.

Introduction

There are many scientific and industrial situations in which on-line monitoring of molecular weight during polymerization reactions would be of great value. These include milliliter-scale experiments in which new polymers are synthesized, pilot plant studies used for process optimization and scale-up of production, and on-line process control in large-scale industrial reactors. On-line monitoring with coupled light scattering and concentration detection yields a continuous record of the weight-averaged molecular mass $M_w(t)$, as a polymerization reaction proceeds. $M_w(t)$ is usually the most important *single* parameter in characterizing a polymer reaction. The time-dependent "signature" of the reaction is also obtained, which may be used to determine reaction rates and mechanisms and to quantitatively explore the effects of different reaction conditions.

The current work grows out of our continuing program to develop real-time monitoring techniques and models for time-dependent phenomena in polymer solutions. Much of our previous work has focused on the use of time-dependent static light scattering (TDSLS) to characterize depolymerization reactions caused by enzymes, ultraviolet radiation, and acids and bases.[1−4] Depolymerization reactions are not mere time reversals of polymerization reactions, however, and the chemical conditions involved and kinetics and mechanisms are in general quite different. Hence, both the technical aspects of monitoring polymerization vs depolymerization and the theories used for describing the respective processes are quite distinct.

This work lays out the chief issues in making real-time polymer mass determinations in homogeneous polymerization reactions in solution and presents a coupled series of instruments used to achieve this. Extensive data from the polymerization of poly(vinyl pyrrolidone) (PVP) are presented as a demonstration of the technique. The technique as presented here is applicable to situations where monomer is dissolved in a solvent up to arbitrarily high concentrations, as well as bulk polymerization from pure monomer, where no solvent at all is involved. Hence, the technique should be immediately useful for a broad spectrum of reactions. Future work will deal with the problems associated with heterogeneous reactions.

It is worth pointing out here the potential place of this technique in the arsenal of polymer solution characterization techniques. As a nonequilibrium application, the technique's over-riding advantage will be as a real-time, or quasi-real-time, monitor of polymer kinetic processes. Its biggest weakness is that it gives only the weight averaged mass, M_w, the reduced viscosity, η_r, and the *z*-averaged radius of gyration, $\langle S^2\rangle_z$ (if larger polymers are produced), and provides no direct polydispersity information. On the other hand, the kinetic curves produced on-line should yield information concerning rates and mechanisms. At the industrial level, the time-dependent signatures of the reactions may well serve to indicate problems in mixing, heterogeneity, unexpected kinetics, reaction failure, etc., and even allow for corrective measures to be taken during the polymerization. Furthermore, for well-characterized polymers, for which the dependence of η_r and $\langle S^2\rangle$ on M is well-known, measures of polydispersity may also be obtained on-line by combining the viscosity and light scattering data.

Currently, one of the best techniques for characterizing polydisperse polymers is size exclusion chromatography (SEC, also referred to as GPC, or gel permeation chromatography) coupled with a light scattering detector, a refractometer (or other concentration detector), and, optionally, a viscometer. This allows the detailed mass distribution of a polymer population to be obtained.[5,6] The drawbacks of SEC, however, are that there is a considerable lag-time between injecting a sample and detecting the fractions in the detector

* To whom correspondence should be addressed

10.1021/ma980876e CCC: $15.00
Published on Web 09/24/1998

stream and that the sampling rate of the reaction is rate-limited by the time spread of the separated fractions. Considering also the cost, selection, and maintenance problems of columns, as well as potential overload when worked with repetitive incoming samples of material of imperfectly controlled concentration, SEC is not well-suited as a real-time technique.

Since the focus of this work is the presentation of the technique itself, only a minimum consideration has been devoted to the problems associated with interpreting the time-dependent signatures in terms of kinetic models. A considerable body of literature exists on polymerization kinetics.[7−15]

Preliminary Considerations

Scattering Equation and Restrictions on Reactant Concentration. Most homogeneous polymerization reactions use high starting concentrations of monomer, often up to 100%. When static light scattering intensities are extrapolated to zero scattering angle ($q = 0$), the weight-average molecular weight, M_w, and second and third virial coefficients, A_2 and A_3, respectively, are related via the Zimm approximation,[16] to second order in concentration for dilute or semidilute solutions by

$$\frac{Kc}{I(q=0)} = \frac{1}{M_w} + 2A_2c + 3A_3c^2 \tag{1}$$

where $I(q = 0)$ is the absolute excess Rayleigh scattering ratio of the polymers (i.e. total solution scattering minus the pure solvent scattering level at $q = 0$), c is the polymer concentration in g/cm^3, and K is a constant, given for vertically polarized light by

$$K = \frac{4\pi^2 n^2 (\mathrm{d}n/\mathrm{d}c)^2}{N_A \lambda^4} \tag{2}$$

Here n is the index of refraction of the pure solvent, λ the vacuum wavelength of the incident light source, N_A is Avogadro's number, and dn/dc is the differential refractive index of the polymer in the pure solvent (in cm^3/g). The magnitude of the scattering wave vector q, has its usual definition:

$$q = \frac{4\pi n}{\lambda} \sin(\theta/2) \tag{3}$$

where θ is the angle at which the scattered light is measured.

Equation 1 shows that at high concentrations, where the A_2 and A_3 terms dominate, the scattering from the solution will not vary appreciably in time as M_w increases. *Hence, it is fruitless to attempt monitoring the polymer mass directly on a polymerization reaction carried out at high concentration. The solution must be diluted in order to make meaningful measurements.* Because values of A_2 are either known or easily determined, and those for A_3 less commonly known or evaluated, it suffices to define "high concentration" in terms of A_2. A polymer solution will be too concentrated for useful TDSLS monitoring if

$$2A_2cM_w \gg 1 \tag{4}$$

The acceptable values of $2A_2cM_w$ in practice will depend on the signal-to-noise ratio of the light scattering detection apparatus and the precision to which A_2 is known. In general, there is a weak dependence of A_2 on M for coil polymers. For random coils with excluded volume $A_2 \propto M^{-0.2}$.

Definitions of M_w for Step Growth and Chain Polymerization Mechanisms. It is important at the outset to consider the traditional distinctions between how M_w is defined for step-growth reactions and for chain propagation reactions.[14]

In step-growth reactions (e.g. Nylon, polyamides, and polyesters) all monomers and polymer chains can react with each other and continue propagation until some terminating or capping reaction occurs. In these reactions there is a rather smooth buildup of chain sizes, including dimers, trimers, etc., as the reaction proceeds, so that in computing M_w *the monomers are counted in the average*:

$$M_w'(t) = u\frac{\sum_{i=2}^{\infty} i^2 N_i(t) + N_1(t)}{\sum_{i=2}^{\infty} i N_i(t) + N_1(t)} = u\frac{\sum_{i=2}^{\infty} i^2 N_i(t) + N_1(t)}{N_1(0)} \tag{5}$$

where u is the mass of a monomer (assumed to change insignificantly once incorporated in a polymer), $N_i(t)$ is the number concentration of polymers containing i monomers, and $N_1(t)$ is the number concentration of monomers. It is important to note that $M_w'(t)$ is the average measured directly when the total concentration (monomer plus polymer) is used as c in eq 1, and I is taken as the total solution scattering minus the pure solvent scattering. *Hence, the weight average mass for step-growth polymerization can be determined with a single total concentration detector (e.g. an RI) and a TDSLS detector.*

In chain-growth polymerization, monomers are added successively to the ends of growing chains. This leads to a bimodal distribution, whereby there is a decreasing population of monomer, and a growing polymer population, whose average masses are relatively large and highly separated from the monomer mass. For these reactions, the concentration of monomer $N_1(t)$ is excluded and, $M_w(t)$ is determined by

$$M_w(t) = u\frac{\sum_{i=2}^{\infty} i^2 N_i(t)}{\sum_{i=2}^{\infty} i N_i(t)} \tag{6}$$

To obtain this average, the c in eq 1 must be the concentration of polymer, that is, the total concentration minus the monomer concentration, and I must be the total scattering minus that when monomer is present. *To determine the polymer concentration, it is necessary to measure both total concentration (e.g. with an RI detector) and monomer concentration (e.g. with a UV detector),* unless a single detection technique can be found which is only sensitive to polymer. Alternatively, industrial chain polymerizations often involve a "flashing reaction" in which monomer and solvent are volatilized, leaving 100% polymer in the process train. This

material might then be diluted with pure solvent, and only one concentration detector would be needed.

It is pointed out that the $M_w(t)$ is the weight average of all active radicals plus accumulated dead chains in the reaction up until time t. Thus, in comparing with kinetic theories, which are often formulated in terms of instantaneous degrees of polymerization, it will be necessary to integrate the theoretical instantaneous values.

Materials and Methods

PVP Polymerization Reaction. The reaction for producing PVP was chosen for its ease of preparation as a first demonstration of the TDSLS technique. Because it is a chain-growth type of reaction, however, the detection procedure is experimentally more demanding, since both polymer and monomer concentration must be simultaneously monitored.

All $M_w(t)$ in this work are computed according to the definition of eq 6. The reactions took place in a solution of pH ~9.5, controlled by ammonium hydroxide (0.3%), per the procedure of Fikentscher and Herrle.[17] Solutions of 20% volume/volume 1-vinyl-2-pyrrolidinone, VP (Sigma Chemical Co., used as received), and ammonium hydroxide in water were first sonicated and placed under vacuum to remove gas and then heated to the appropriate temperature (T = 50 and 70 °C were used) in a round-bottom flask, using a water bath. The temperature inside the reaction flask was monitored by a k-type thermocouple connected to an A/D converter and a computer. A magnetic stirring bar was used inside the flask. The reaction volume was 150 mL. The reaction mixture was withdrawn from the reactor through a PEEK or Teflon tube and mixed with identical solvent, without the VP, by a gradient programmer (ISCO model 2360). An HPLC pump (ISCO model 2350) was used for pumping out the resultant dilute solution from the programmer. After the RI and LS detectors stabilized, hydrogen peroxide was added to start the reaction. Thermocouple data showed that addition of the H_2O_2 (up to 0.8 vol % of the total solution), originally at room temperature, had no noticeable effect on the temperature of the bath, which was stable to within ±1 °C. All solutions were filtered through a 0.22 μm filter (Millipore) before using. The reactions generally ran to 100% monomer conversion or otherwise were stopped by bringing down the temperature and/or by dilution of the final product.

As stated, the reaction used a starting concentration of vinyl pyrrolidone monomer of 20%. An initial attempt at measuring the light scattering for a PVP reaction at this concentration showed almost no measurable variation in the scattered intensity as the reaction progressed. This is consistent with the above discussion concerning the need for dilution. Measurements in our laboratory on both PVP products from this work and commercially available fractions of various M_w yield an approximate expression of (ignoring the relationships between the different averages involved)

$$A_2(\text{mol cm}^3/g^2) = (5.52 \times 10^{-3})M^{-0.21} \qquad (7)$$

For a value of $A_2 \sim 6.9 \times 10^{-4}$ at $M_w = 2 \times 10^4$ g/mol and c = 0.300 g/cm^3 (a typical reaction concentration), $2A_2cM_w = 8.3$; i.e., changes in the term $1/M_w$ in eq 1 are quite small compared to the second term, which would usually render such measurements unreliable. The $3A_3c^2$ term from eq 1 will make the situation even worse.

Postreaction SEC measurements of final product were made using equipment previously described and analyzed in detail.[5,6]

Dilution and Handling of Reacting Solution. An ISCO 2360 programmable gradient mixer was used to withdraw a small flow of reacting solution and mix it with a much larger flux of pure solvent from a reservoir to produce a diluted reaction solution. The output of the mixer was withdrawn by an ISCO 2350 HPLC isocratic pump, which then fed the detectors arranged in series. These were a light scattering flow chamber, which we designed and built; an ultraviolet absorbance detector; a single capillary viscometer, which was also constructed in our laboratory; and a refractive index detector (Waters 410), as described below. Between the pump and the detectors was a 0.5 μm SEC in-line frit-type filter. This considerably reduced light scattering spikes in the raw data, as the data presented here show.

It is noted that the mixer nominally withdraws preset percentages of two different solutions via a piston and then pumps them to a mixing chamber of about 1 mL. The percentages are determined, however, according to the time interval of withdrawal from each solution during one piston withdrawal cycle. The nominal percentages will be obtained only if each solution has roughly the same viscosity. The initial 20% VP in water solution is already about twice as viscous as water, and the viscosity increases strongly as the polymerization reaction proceeds. Because, according to the manufacturer, the piston is not highly sealed, there are significant leaks, which can make the actual piston suction vary strongly with the viscous resistance of the solvent being pulled. This, together with the effect of increasing solution viscosity, reducing flow rate, means that *the actual concentration of reacting solution withdrawn will steadily diminish below the nominal value as the polymerization reaction proceeds. It is hence necessary to follow the concentration of the diluted solution with an appropriate on-line concentration detector.* It is important to point out that variations in concentration reaching the detector during the reaction do not impair the technique in any way, since the computations of M_w are made using the ratio of I and c, and a small A_2 correction involving c. The technique is hence quite robust in the face of changes in the reactor viscosity as polymerization proceeds.

Concentration Detectors. An RI detector was chosen in this work as the on-line detector for total concentration. We found the measured value of dn/dc for PVP and VP to be the same, 0.173 in water at T = 25 °C and λ = 633 nm. A Waters 410 was chosen, since it has the capability of working at higher concentrations than are normally used in SEC applications. Concentrations were chosen to be in the range of 0.001−0.01 g/cm^3. SEC concentrations are usually 2−3 orders of magnitude smaller, since fractionation occurs in the separating columns. In this work, smaller concentrations could indeed have been used, but there is little disadvantage in maintaining higher concentrations (which are nonetheless still quite dilute) so that polymer mass can be followed even at the early stages of polymerization. The RI detector was thermostated to 30 °C and showed no detectable drift over the course of the experiments.

The VP monomer has a UV absorption peak at about 240 nm (molar absorption coefficient ~ 8000 M^{-1} cm^{-1}), which disappears upon polymerization, as the vinyllic double bond is lost. Hence, a UV detector equipped with a flow cell provided an excellent means of following monomer concentration with time, that is $m(t)$. A Shimadzu SPD-10AV with a 0.1 mm path length flow cell was used. Even with this short path length, the absorbance was too high at the peak, so absorption was monitored off-peak at 265 nm.

Lag-Time Considerations. An important parameter determining whether the on-line technique can be used as a *real-time* technique, is the lag-time between material flowing from the reaction vessel to the detectors. That is, the detectors measure the diluted reaction solution in "detector time", t_d, which measures the state of the reactor at an earlier "reactor time", t_r, which is equal to the detector time minus the instantaneous lag-time. This lag time consists of the lag time from the reactor to the mixing chamber, which can increase in time as the reactor solution viscosities, plus a constant lag time from the mixing chamber to each detector. When lag-time is minimized to the point that $t_d \sim t_r$, then the technique can be considered to monitor polymerization in real-time.

There is a volume of tubing, v_{pol}, between the reactor and the mixing chamber. Since the reaction mixture is being withdrawn at a fairly slow rate compared to the pump rate

(4% of the pump flow rate of 1.5−2 mL/min), it takes a lag-time of

$$\tau = v_{pol}/(fQ) \tag{8}$$

where f is the fraction of polymerizing solution being withdrawn for mixing and Q is the flow rate leaving the mixer. The tubing in the current system had $v_{pol} = 0.47$ mL. For $f = 0.04$ and $Q = 2$ mL/min, this gives a lag-time of about 5.9 min. As f decreases with time, this lag-time grows longer. While no attempt has been made to minimize the lag-time in this demonstration project, it is clear that there are a number of parameters available for lowering this significantly: reduce the diameter of the feeder and mixer tubing, increase the overall flow rate, and/or increase the percentage of reaction mixture being withdrawn. It should be possible in practice to bring the lag-time down to under 1 min if required. In this work, a reaction at a nominal $f = 0.04$, running for 300 min at 2 mL/min consumed 24 mL of reactant solution.

The effect on lag-time of diminishing concentration being withdrawn from the reactor as polymerization proceeds can be dealt with in a precise fashion, on-line, as follows: The time it took for a mass element of withdrawn reaction fluid to traverse a length of tubing L and arrive at a detector at detector time, t_d, is denoted as $\tau(t_d)$, and is given by

$$L = \int_{t_d-\tau(t_d)}^{t_d} v(t')\, dt' \tag{9}$$

where $v(t')$ is the fluid element's velocity at time t' and A is the cross-sectional area of the tube. Now $v_{pol} = AL$ is the volume the element traverses before being mixed with the solvent, and $v(t')A = f(t')Q$ is the flow rate of the fluid withdrawn from the reactor. Since $f(t_d) = C(t_d)/m_o$, where m_o is the initial monomer concentration in the reactor (a constant)

$$\frac{v_{pol} m_o}{Q} = \int_{t_d-\tau(t_d)}^{t_d} C(t')\, dt' \tag{10}$$

For discrete measurements of time and concentration, as are collected in this on-line monitoring technique, the lag-time at detector time point $t_{d,i}$ is determined from

$$\frac{v_{pol} m_o}{Q} = \Delta t \sum_{j=(t_{d,i}-\tau_{t_{d,i}})}^{t_{d,i}/\Delta t} C_j \tag{11}$$

Δt is the time interval between successive points and is usually constant (usually 1 to 3 s in this work). The correspondence between $t_{d,i}$ and the reaction time point $t_{r,i}$ is

$$t_{r,i} = t_{d,i} - \tau_{t_{d,i}} \tag{12}$$

Because the RI detector permits on-line determination of $C(t)$, it is a simple matter to form the sum of C_j to find the τ_{t_i} that satisfies eq 11 at each point. The reaction time can hence be computed at every detector time point as the data are collected.

The volume from the start of the mixing chamber to the detector chain was about 2 mL, so that data only need be shifted a constant amount of 1 min (at 2 mL/min) due to this additional volume. This small, additional lag-time, further subtracted from $t_{r,i}$ in eq 12, does not change with $f(t)$, since it depends only on Q, which remains constant throughout the reaction. Likewise, there was an interdetector dead volume of 1 mL between the TDSLS unit and the UV detector, 0.15 mL from the UV detector to the viscometer, and 0.16 mL from the viscometer to the RI detector.

Mixing of the sample due to lateral diffusion and a parabolic (Poisseuille) flow profile during withdrawal of the reaction mixture should also be considered. This was assessed empirically by injecting a 10 μL sample of end-product PVP at about 10 mg/mL into the reactor withdrawal tube and measuring the half-width of the peak produced upon arrival at the refractometer. The half-width for a lag-time of 400 s was about 70 s. The sampling time in all experiments was typically between 1 and 3 s per point, so that there is appreciable mixing in adjacent sample points. The reactions typically lasted on the order of 10 000 s in detector time, so that there are over 100 complete mixing widths measured per experiment, giving a good resolution for the reactions. Decreasing lag-time would increase this resolution even further.

Single Capillary Viscometer. A single capillary viscometer was placed after the light scattering chamber to measure the viscosity of the diluted solution in real-time. A capillary of radius 0.01 in. was used, and each end was connected to one side of a differential pressure transducer (Validyne Corp.) via T-connectors. The voltage output of the pressure transducer is directly proportional to the pressure drop across the capillary. The viscosity is directly related to the measured pressure drop across the capillary via the Poisseuille equation, which gives the flow rate Q (cm^3/s) of a liquid of viscosity η through a capillary of length L and radius R, under a pressure difference ΔP:

$$Q = \frac{\pi R^4 \Delta P}{8\eta L} \tag{13}$$

Solution viscosity is given in terms of polymer concentration c, by

$$\eta = \eta_s(1 + [\eta]c + \beta[\eta]^2 c^2 + ...) \tag{14}$$

where η_s is the viscosity of the pure solvent, $[\eta]$ is the intrinsic viscosity of the polymer, and β is a hydrodynamic constant, usually equal to about 0.4 for neutral, random coil polymers. Reduced viscosity, η_r, is determined directly from the measured voltage $V(t)$, without need of a calibration factor via

$$\eta_r(t) = \frac{V(t) - V(\text{pure solvent})}{c(t)V(\text{pure solvent})} \tag{15}$$

Intrinsic viscosity $[\eta]$ is the limit of $\eta_r(t)$ as polymer concentration c goes to zero. For non-Newtonian fluids, which many polymer solutions are, the limit of the shear rate, $\dot{\gamma}$, must also go to zero to find $[\eta]$. In capillary viscometers $\dot{\gamma}$ is never zero, and the average value is given by

$$\dot{\gamma}_{ave} = \frac{8Q}{3\pi R^3} \tag{16}$$

Average shear rates can actually be quite high. For the current system $\dot{\gamma}_{ave}$ at 2 mL/min is 1727s^{-1}. Shear rate effects for polymers fall off dramatically as concentration is decreased.

For PVP, the intrinsic viscosity was measured to be:[18]

$$[\eta] = 0.18M^{0.46} \tag{17}$$

Light Scattering Flow Chamber and Detection. A scattering chamber was constructed from black nylon round stock. A channel was bored concentric with the round stock, and fittings were made to accommodate standard HPLC connectors. Borosilicate windows (Edmund Scientific) of 5 mm diameter were fastened into holes in the side of the chamber to let in the incident beam and let out the exit beam. The beam of a 25 mW vertically polarized diode laser operating at a wavelength of 677 nm was focused through the window and at the center of the chamber using an $f = 7$ cm lens. A single hole was made at $\theta = 90°$ for detection, and a Polymicro Technologies optical fiber (FIP 400 440 480) was epoxied in. The half-angle of acceptance (also termed the numerical aperture) of the fiber is given by

$$\theta_A = \sin^{-1}\left(\frac{\sqrt{n_c^2 - n_{cl}^2}}{n_s}\right) \tag{18}$$

where n_c and n_{cl} are the refractive indices of the core and

cladding, respectively, and n_s is the refractive index of the liquid in which the fiber is immersed. The Polymicron fiber has $\theta_A = 0.22$ rad (12.6°) in air, 0.165 rad (9.4°) in water, and 0.147 rad (8.4°) in toluene.

The scattering volume v_{LS} detected by the fiber is

$$v_{LS} = \int_{z_1}^{z_2} A(z)\, dz \tag{19}$$

where $A(z)$ is the cross-sectional area of the laser beam as a function of distance along the laser beam direction of propagation, z. z_1 and z_2 are the cutoff limits of the laser beam which enter the optical fiber, where

$$|z_2 - z_1| = D + 2R \tan(\theta_A) \tag{20}$$

D is the core diameter of the fiber, and R the distance of the fiber to the center of the laser beam, which in this chamber is equal to the chamber radius.

Taking the average beam waist of the unfocused diode laser as $d = 2$ mm, and applying the Gaussian beam approximation $w \approx \lambda f/d$ to estimate the focused beam width, w, yields a scattering volume of 16.2 nL in water, and 17.7 nL in toluene.

The total power entering the optical fiber, P_t, can be computed as follows. Choose the center of the optical fiber face as the origin, and let $\mathbf{r}$ identify any point on the plane of the fiber's face, where $\hat{n}$ is the unit normal to the fiber face. The scattering power emanating per unit volume in the scattering volume is $\rho(\mathbf{r}')$, where $\mathbf{r}'$ is the vector locating an infinitesimal volume element in the beam. Then P_t is found by integrating the power from each infinitesimal beam volume, which diminishes as $1/[\vec{r} - \vec{r}']^2$, over both the surface of the optical fiber face and over the entire scattering volume

$$P_t = \int\int \frac{\rho(\vec{r}')\hat{n}\cdot(\vec{r} - \vec{r}')}{|\vec{r} - \vec{r}'|^3}\, d^3r'\, d^2r \tag{21}$$

If the average beam waist is much smaller than R if $\theta_A \ll 1$ rad, and if $D \ll R$, then the above integral is well approximated by

$$P_t \cong \frac{\pi w^2 A \rho}{4R^2}(D + 2R\theta_A) \tag{22}$$

where A is the area of the fiber face and ρ the average scattered power density in the scattering volume. When $2R\theta_A \gg D$, P_t is inversely proportional to n_s. The relative scattering from two solvents of different n_s is given as a geometrical optical correction factor

$$F(1,2) = \frac{D + 2R \tan(\theta_{A,1})}{D + 2R \tan(\theta_{A,2})} g \tag{23}$$

where a reflection loss term g is given by

$$g = \frac{\left(1 - \left|\frac{n_1 - n_c}{n_1 + n_c}\right|^2\right)}{\left(1 - \left|\frac{n_2 - n_c}{n_2 + n_c}\right|^2\right)} \tag{24}$$

The exit end of the detection fiber was fixed in front of a Hammamatsu S1406-4 photodiode, and an additional DC 1000× amplification stage was used on the photodiode output (supplied by Brookhaven Instruments Corp.).

Absolute light scattering intensities were determined according to

$$I(t) = \frac{(V(t) - V_{solvent})}{(V_{toluene} - V_{dark})} F(toluene,solvent) I_{toluene} \tag{25}$$

where $V_{solvent}$ is the scattering voltage level from the solvent, $V(t)$ is the time dependent scattering voltage from the polymerizing solution, and $I_{toluene}$ is the absolute Rayleigh scattering ratio of toluene. Extrapolating the value of Bender et al.[19] to 677 nm via the inverse λ^4 yields $I_{toluene} = 1.069 \times 10^{-5}$ cm^{-1}.

Table 1. Calculated Geometrical Correction Factor, Reflection Loss, and Measured Relative Scattering Values of Standard Solvents Compared to Ref 19

solvent	$g_{toluene/solvent}$	$F_{toluene/solvent}$	$R_v(90°)_{solvent}/R_v(90°)_{toluene}$		deviation (%)
			Bender et al.[19]	our data	
CCl_4	0.976	0.957	0.447	0.471	5.55
C_6H_{12}	0.982	0.946	0.390	0.378	−2.97

Stray light is the single biggest problem in static light scattering. The problem is most acute when an absolute reference solvent is used, such as toluene in eq 25, to determine the absolute excess Rayleigh ratio of the polymer in solution. Whereas time independent stray light (e.g. from a scratch on a window) will be subtracted in the numerator of eq 25 (because it is present when both $V_{solvent}$ and $V(t)$ are measured), it will not be subtracted out in the denominator, $V_{toluene} - V_{dark}$. Any stray light present will add directly into the value of $V_{toluene}$, thus lowering the computed value of $I(t)$. *As a consequence, all polymer molecular masses measured will be systematically underestimated when stray light is present.*

To determine if stray light is present in a single angle chamber, it is possible to measure the relative scattering from several materials of known Rayleigh scattering ratio. The ratios in our scattering chamber must be corrected by $F(1,2)$ of eq 23. In Table 1 our values have been compared with those of Bender et al. As can be seen, the deviations are on the order of a few percent. However, it is worth noting that the results of ref 19 displayed differences of up to 10% compared to other authors.

An estimate of the amount of stray light can be made as follows. Let V_t and V_x be the true baseline-subtracted scattering voltages for toluene and another solvent whose absolute Rayleigh scattering ratio is known. Let $V_t + V_{tf}$ and $V_x + V_{xf}$ represent the voltages actually measured for toluene and solvent x when stray light is present. V_{tf} and V_{xf} are the unknown scattering voltages due to stray light when toluene and solvent x are measured, respectively. The fractional error, Err, between the readings with stray light and those that would be made in the absence of stray light is computed from the readings, by definition, as

$$\mathrm{Err} = \frac{\left(\frac{V_x + V_{xf}}{V_t + V_{tf}}\right) - \frac{V_x}{V_t}}{\frac{V_x}{V_t}} \tag{26}$$

If it is assumed that the stray light for both solvents is roughly equal (this is a good approximation for the solvents in Table 1, since their indices of refraction are quite similar, so that index matching of scratches, etc. should be roughly the same), that is $V_{tf} = V_{xf} = V_f$, then

$$\mathrm{Err} = \frac{\left(\frac{V_t}{V_x} - 1\right)}{\left(\frac{V_t}{V_f} + 1\right)} \tag{27}$$

so that the stray light, as a fraction of voltage from pure toluene with no stray light, is

$$\frac{V_f}{V_t} = \frac{\mathrm{Err}}{\frac{V_t}{V_x} - 1 - \mathrm{Err}} \tag{28}$$

The error due to stray light may account for only a fraction of the deviation between our measured values and reference data shown in Table 1. As these deviations are much smaller

than 10%, it is concluded that stray light is immeasurably small in the experiments in this work.

It is worth noting that in a traditional, single detector SLS goniometer, to determine whether stray light exists, it is sufficient to require that the relative scattering intensity of a Rayleigh scatterer (e.g. toluene) times the sine of the scattering angle (to correct for increased scattering volume moving away from $\theta = 90°$) be constant, typically to within 1%, over the range of measured angles. For a multiangle, multidetector instrument, it is possible to determine whether stray light exists by measuring the ratio of the relative excess scattering of a Rayleigh scatterer in a solvent (e.g. low mass polystyrene in toluene) to that of the pure solvent (e.g. $V_{\text{toluene}} - V_{\text{dark}}$). The ratio should be the same at each angle if no stray light is present.

The use of a single detector at $\theta = 90°$ is justified in this work, and in any case where $q^2\langle S^2\rangle \ll 1$. At any rate, it is straightforward to add extra angles to the chamber so that $\langle S^2\rangle_z$ can also be measured for polymers attaining larger sizes. In this study the PVP attains maximum M_w on the order of 150 000 g/mol. Reference 18 gives for PVP

$$\langle S^2\rangle^{1/2}\,(\text{Å}) = 0.73M^{0.45} \tag{29}$$

where M is in g/mol. For $M = 150\,000$, $\langle S^2\rangle^{1/2} = 155$ Å, so that $q^2\langle S^2\rangle = 0.07$, using a fixed scattering angle of 90° and a vacuum wavelength of 677 nm. Hence, to an excellent approximation, we use the form of eq 1 with $P(q) = 1$, that is

$$\frac{1}{M_{w,ap}} = \frac{Kc}{I(\theta = 90°)} = \frac{1}{M_w} + 2A_2c \tag{30}$$

where $M_{w,ap}$ is the apparent weight averaged mass, which results from $Kc/I(\theta = 90°)$, without correcting for A_2. The true weight average mass M_w is computed directly from eq 30 when A_2 is known. The fractional systematic error in M_w, due to an uncertainty ΔA_2 in A_2, is

$$\frac{\Delta M_w}{M_w} = 2cM_w\Delta A_2 \tag{31}$$

A point worth noting for chain polymerization is that there is a bimodal population of monomers and polymers interacting. A more rigorous approach would be to treat this as a binary system and use the standard multicomponent scattering formalism.[20,21] This requires knowledge of the excluded volume between a monomer and a chain. The net effect of this treatment will be to use $c = C_p + \alpha m$ in eq 30, where C_p is the polymer concentration, m is the monomer concentration and α is an integration constant related to the ratio of excluded volume between a monomer and chain and between a chain and another chain. Because $2cM_wA_2$ is small for the experiments in this work, we lump C_p and m together with $\alpha = 1$ in eq 30, as a reasonable first approximation.

Another related point is that in computing the excess scattering due to the polymer, the intensity due to monomer before the reaction is subtracted from the total intensity. As the reaction proceeds, one would normally have to correct this subtraction for the diminishing amount of monomer present. In reality, however, the monomer excess over the pure solvent was only a few percent of the pure toluene scattering (the reference solvent) and represented typically less than 1% of the total final scattering signal, so that no appreciable error is introduced by defining the excess scattering intensity at any moment to be the total scattered intensity minus that from solvent and monomer before polymerization began.

The RI, viscometer, UV, thermocouple, and light scattering signals were captured by a Data Translation DT2801-A analogue to a digital converter seated in the backplane of an IBM 80386 PC, using custom-written software.

Results and Discussion

Figure 1 shows raw voltage data vs detector time t_d, for the RI, UV, TDSLS, and viscometer for a typical PVP

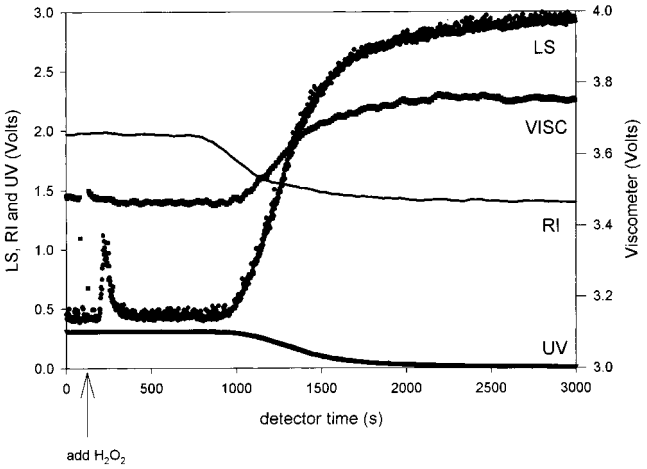

Figure 1. Raw detector voltages vs detector time, t_d, for a PVP reaction (2 in Table 2). RI, UV, TDSLS, and viscometer signals are shown.

polymerization. The data are for reaction 2 in Table 2. The reaction was initiated at $t = 200$ s by briefly stopping the pump and adding 0.5 mL of H_2O_2, giving $[H_2O_2] = 0.098$ M. A break in the viscometer signal is seen at the moment of injection followed shortly thereafter by a light scattering spike. The mix set on the gradient programmer was 4% reacting solution and 96% pure solvent (water with 0.3% ammonia). The pump flow rate for the mixed, diluted reaction stream was 1.5 mL/min, so that the nominal extraction rate from the reacting solution was 60 μL/min.

Figure 2 shows the total concentration of the reactant stream, c, passing through the detectors, taken from the RI data in Figure 1, as well as the buildup of the polymer concentration, C_p, obtained from the differences in concentrations measured by the RI and UV detectors. The actual, measured starting concentration was quite close to the nominal concentration of 0.008 g/cm^3 (4% of the 0.200 g/cm^3 VP solution). This confirms that the mixer could produce the nominal value for the starting reactor solution. As seen in Figure 2, however, the smooth decrease in the concentration shows that the rate at which material was withdrawn fell substantially below the nominal rate as polymerization proceeded and the viscosity of the reaction solution increased. As previously explained, this drop in concentration in no way affects the accuracy of the determinations, and in fact increases the accuracy of M_w, since decreasing c means the $2A_2c$ correction term in eq 30 will decrease.

Figure 3 shows the apparent weight averaged mass, $M_{w,ap} = I/Kc$, vs detector time, t_d, as well as the true weight average mass, M_w, obtained from the A_2 correction from eq 30, as previously discussed. The values of A_2 were computed according to eq 7, based on the apparent mass at each point in time. The maximum correction, occurring at the end of the polymerization, is only about 23%. From eq 30 (error on M due to error in A_2), a 10% error in A_2 will produce only a 2.3% error in the corrected final mass. (The value of α is irrelevant at the end since $m = 0$.) The mass of highly scattered points before about 1000 s correspond to the large error in computing M_w, when both c and I in eq 30 are extremely small. Random errors are considered below.

Figure 4 shows the true mass from Figure 3 plotted both vs detector time, t_d, and reactor time, t_r. For visual clarity in overlapping the curves, the small spikes inherent in the data, and shown in Figure 3, have been

Table 2. List of Polydispersity Index M_z/M_w and Final M_w for a Series of Reactions[a]

reaction no.	$M_{w,final}$	M_z/M_w	$M_{w,SEC}$	M_w/M_n	T (°C)	[VP]/[H_2O_2] (M/M)[b]	notes[c]
1	17 000				70	9.5	
2	34 000				70	18.4	
3	16 000	2.55	14 500	4.4	70	9.5	
4	101 000	2.55	102 000		70	47.4	
5	26 000	2.53	19 500	5.0	50	9.5	
6	25 000	2.46	22 600		50	9.5	aliquots withdrawn
7	41 000	2.7	53 400	4.5	70	42.1/4.7	two H_2O_2 injections
8	900 000				70	474	dead-end

[a] [VP] was 20 volume % in all reactions. [b] Bottled H_2O_2 was nominally 25−35% H_2O_2. The value quoted is the directly measured volume (i.e. assuming 100%). [c] All reactions went to 100% conversion of monomer, except 8, which ended after 71% conversion.

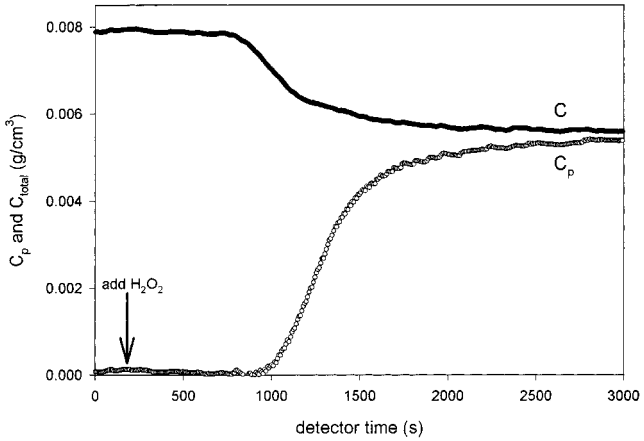

Figure 2. Total concentration of the diluted solution (C) vs t_d for reaction 2 (from data in Figure 1). Also shown is the concentration of polymer, C_p.

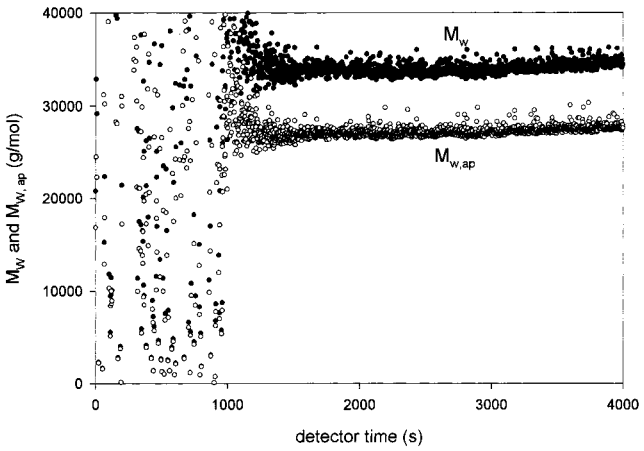

Figure 3. Apparent weight averaged molecular mass, $M_{w,ap}$, and A_2-corrected M_w. Raw data were from Figure 1.

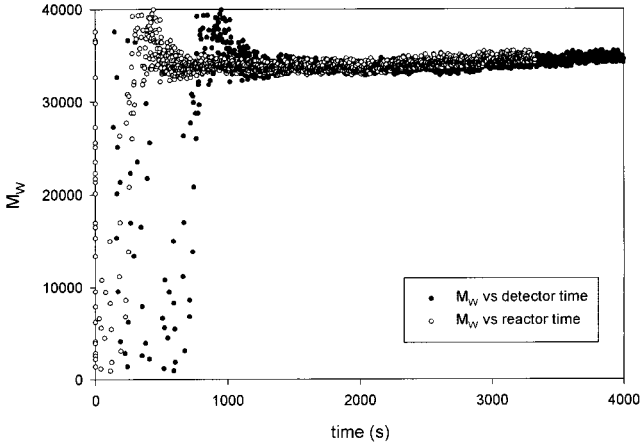

Figure 4. M_w vs detector time and vs reactor time for the data from Figure 1.

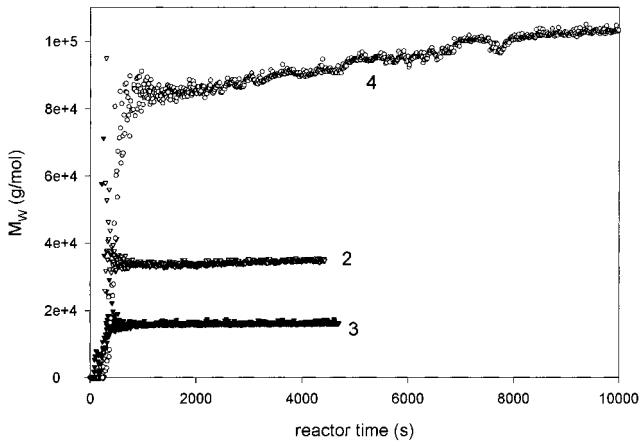

Figure 5. M_w vs reactor time for several experiments (reactions 2−4). Conditions are listed in Table 2.

eliminated in Figure 4. Because of the lag due to a finite amount of tubing between the reaction vessel and the detectors, these two times are not equal, as explained above. The detectors measure the state of the reactor solution as it was earlier, back in time by an amount equal to the instantaneous lag-time. The instantaneous lag-time was computed according to eqs 11 and 12 above, with $V_{pol} = 0.47$ mL. The lag-time started at 460 s and increased to a maximum of 670 s as the fraction of the flow withdrawn from the reactor continuously decreased in time. Although the shapes of the two curves in Figure 4 are quite similar, they are not quite superposable on each other, because of the changing lag-time, due to the changing withdrawal fraction of the mixing pump as the reaction solution viscosifies in time.

Figure 5 shows M_w vs reactor time for several different reactions at different temperatures and initial H_2O_2 concentrations. The parameters for these different experiments are summarized in Table 2. As expected, increasing the ratio of monomer to initiator increased the M_w. Also, increasing the temperature for a given monomer-to-initiator ratio had the expected effect of increasing the conversion rate and decreasing the M_w. Figure 6 shows M_w vs initial monomer to initiator concentration. It is quite linear, which has consequences for rationalizing the kinetics, which are discussed below.

Figure 7 shows M_w vs conversion, defined as the concentration of polymer divided by the total monomer plus polymer concentration, i.e., the ratio of (RI concentration − UV concentration)/(RI concentration). This type of representation is most commonly used by polymer kineticists. The striking feature in all of the curves in Figure 7 is that M_w attains its final value almost immediately as conversion starts. Experiment

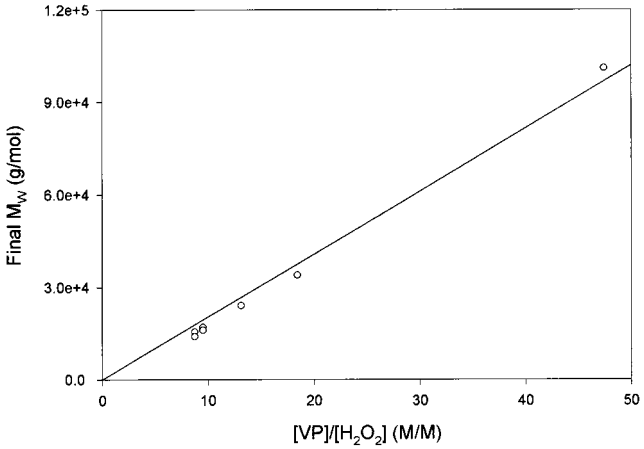

Figure 6. Final M_w vs the ratio of monomer to initiator (M/M) for seven different experiments, which were all performed at 70 °C.

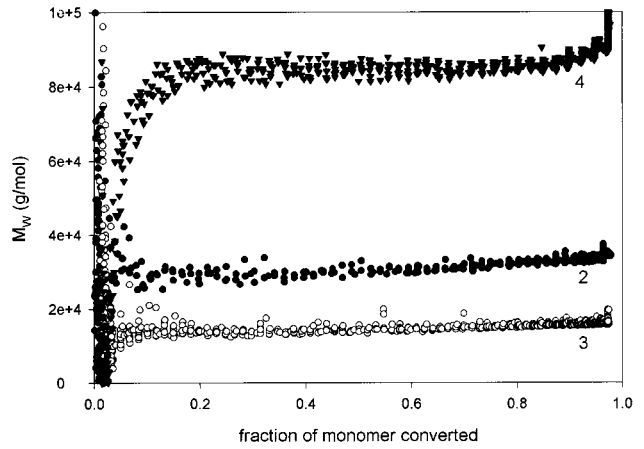

Figure 7. M_w vs fraction of monomer converted to polymer for several reactions.

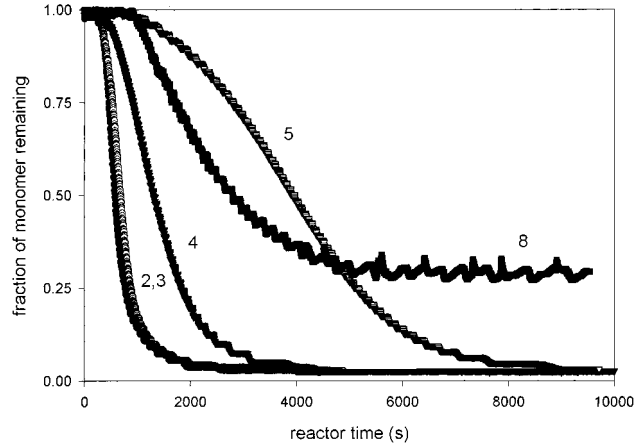

Figure 8. Fraction of monomer remaining vs time for reactions 2−5 and 8. Reactions 2 and 3 have the quickest decay and are virtually indistinguishable in the graph; 8 was a deliberate attempt at dead-end polymerization using extremely low [H_2O_2].

4, however, shows a slight increase in M_w after 90% conversion, which is probably due to viscosity effects, as discussed below. The fact that there is a measurable rise in M_w around 100% conversion suggests that some chain termination might be occurring via recombination.

Figure 8 shows the remaining fraction of monomer vs reactor time for several of the experiments in Table 2. All reactions proceed to complete consumption of

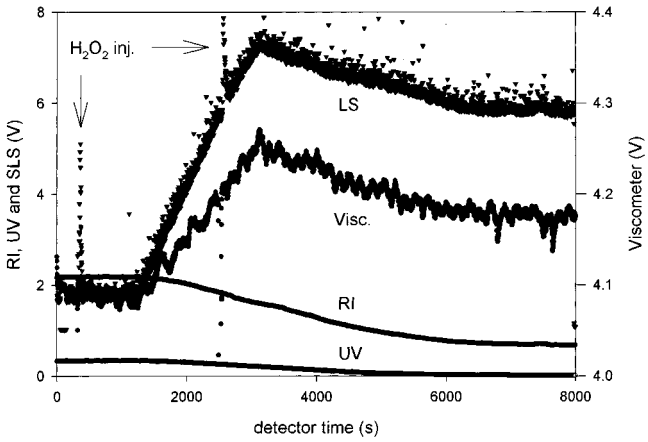

Figure 9. Raw data for experiment 7 in which additional H_2O_2 was injected during the reaction in order to cause a decrease in M_w vs time.

monomer, within the error bars of the UV detector, except for experiment 8. In this latter experiment a dead-end polymerization was attempted. A large ratio of [VP]/[H_2O_2] was used (474 M/M), and the reaction terminated before all monomer was consumed. Also apparent in Figure 8 is the fact that there is what has sometimes been described as a "chemical lag-time" before monomer begins to be appreciably consumed. While most pronounced on curve 5 taken at lower temperature (50 °C), all the experiments showed this effect. It is most likely related to the relationship between the controlling rate constants and initial initiator concentration, as discussed below.

After observing the near constancy of M_w for the various reactions, it was decided that it would be instructive to deliberately change M_w during the reaction. This is equivalent to an on-line adjustment to reaction conditions during the reaction. To make the effect dramatic, additional initiator was added after about 20% of the monomer was consumed. As expected, this decrease in the monomer/initiator ratio immediately led to the production of smaller chains, making M_w decrease in time as the smaller chains became an increasing percentage of the population. Figure 9 shows the raw data for this experiment. Figure 10 (top panel) shows how M_w and viscosity decrease in time after the additional initiator was injected. Figure 10 (bottom panel) shows the polymer distribution $C(M)$ determined by injecting a diluted portion of the final reaction mixture into the SEC. Although the numerical value of M_z/M_w is not much larger than for the other reactions (2.7 vs about 2.5), there is a clear bimodality of masses, which is the deliberate result of the second injection of H_2O_2. A minority of the monomer polymerized to large chains, since the second injection of initiator occurred at only about 20% conversion, so that most of the monomer subsequently polymerized to small chains.

The SEC measurements on several of the end products from the reactions in Table 2 give surprisingly consistent values of the polydispersity factor M_z/M_w, which is around 2.5. The masses determined by SEC were normally close to the on-line measurements.

Figure 11 shows RI results from SEC for an experiment (6 in the table) in which reaction aliquots were frequently withdrawn, diluted, and cooled to preserve the reaction state mixture. The striking result is that the peak value and the shape of the RI chromatograms are essentially the same at any point during the

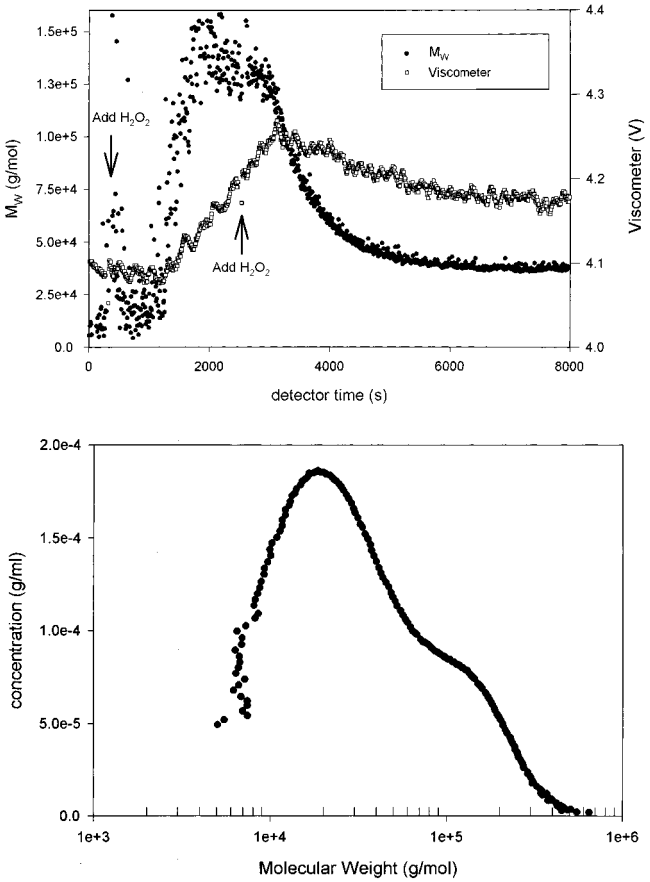

Figure 10. (Top panel) M_w and vs detector time for reaction 7. This clearly shows the subsequent production of short chains after extra initiator was added during the reaction. (Bottom panel) Mass distribution $C(M)$ from SEC, for reaction 7, showing the expected bimodality. A small large population was formed before the second injection of H_2O_2, after which the remaining (~80%) monomer formed short chains.

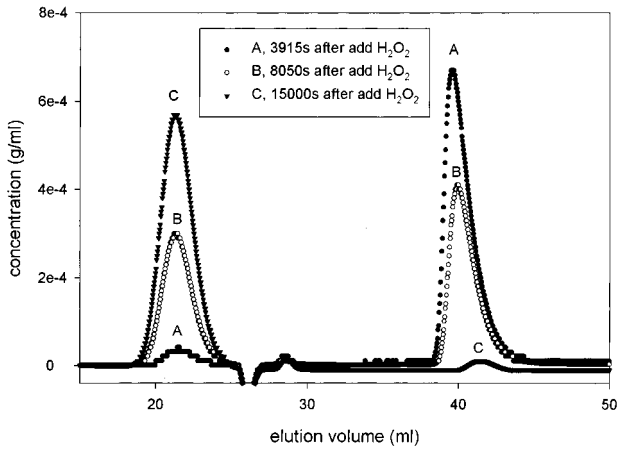

Figure 11. SEC refractometer data vs elution volume for three different times during the reaction 6. The monomer peak can be seen diminishing at the later time point and the polymer peak builds up on the same point, confirming the fact that polymer chains of essentially the same mass and distribution are produced throughout the reaction. In fact, the polymer peaks are virtually superposable on each other.

reaction. (The population is also unimodal, as opposed to the deliberate bimodality of Figure 10 (bottom panel) This confirms the on-line result that M_w quickly reaches a constant value as conversion proceeds. The top portion of Figure 12 shows the polydispersity index M_z/M_w at different points in the reaction, as obtained from

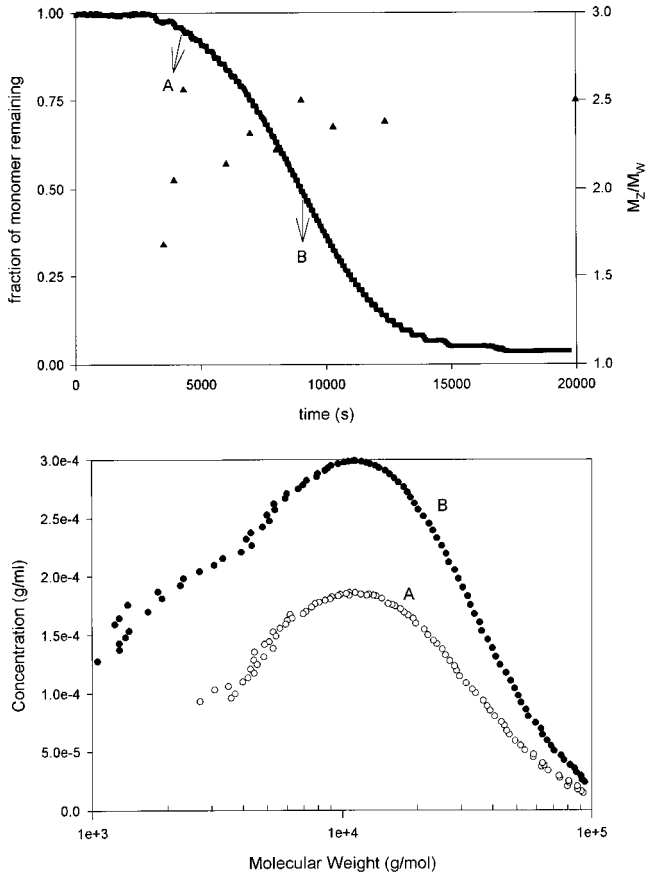

Figure 12. (top panel) Polydispersity index M_z/M_w from SEC (▲) for selected time points for experiment 6. Also shown is the degree of monomer conversion. (bottom panel) Population distribution of polymer $C(M)$ from SEC analysis. The letters A and B show which points in the reaction the $C(M)$ curves were taken from. The virtually identical peak masses confirm the on-line results, which indicate no appreciable change in mass as conversion proceeds for most reactions in the table.

combined RI and light scattering detectors on the SEC. These values quickly rise to a plateau and show no evolution within the rather wide error bars during the rest of the polymerization. The values are quite close to the general value of 2.5 shown in Table 2 for the end-products of other experiments. The SEC also confirmed the time course of the on-line measurements, namely that M_w quickly rose to a plateau value, where it remained as the rest of the monomer was consumed. The lower part of Figure 12 shows the population distribution $C(M)$ of polymer for aliquots taken at the detector times shown by the arrows. The peak positions and widths are virtually identical, the difference in height being simply related to less conversion of monomer to polymer for the earlier time point.

Figure 13 shows the reduced viscosity, defined by eq 15 vs t_d, for the data from reaction 4 in Table 2. In principle, this could also be used as a process control parameter. Furthermore, although in the SEC context, reduced viscosity is often taken as equal to the intrinsic viscosity, it must still be born in mind that the reduced viscosity results, in principle, need to be extrapolated to zero concentration and zero shear. At any rate, intrinsic viscosity is not an absolute measure of M_w, but rather depends on a specific relationship, such as eq 17, which can be fraught with error. While we find M_w determined by light scattering intrinsically superior to an indirect estimate of the molar mass via reduced

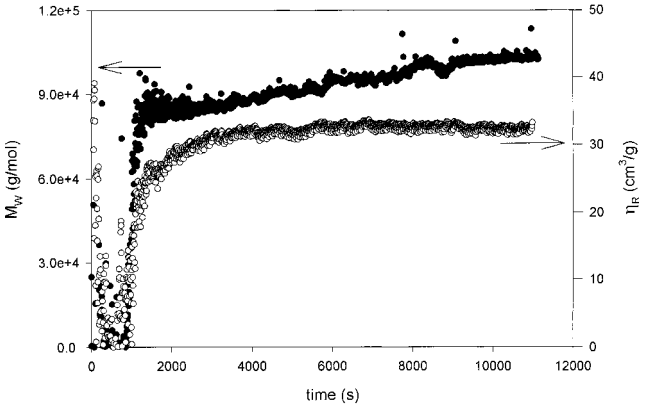

Figure 13. M_w and reduced viscosity η_r vs detector time for reaction 4.

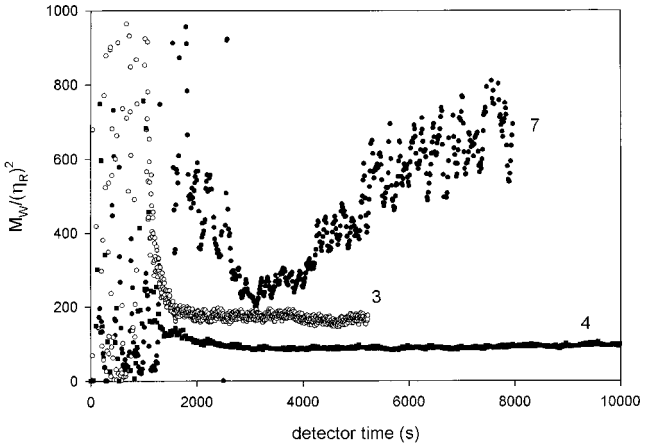

Figure 14. A measure of the polydispersity M_w/η_r^2 for reactions 3, 4, and 7. This quantity is quite constant for reactions 3 and 4, consistent with the SEC results on 6 performed under similar conditions, which shows that polydispersity does not change much during conversion. Reaction 7, on the other hand, received an additional injection of H_2O_2 during the reaction, which should lead to higher polydispersity, as shorter chains are then produced.

viscosity, it may be possible to use the auxiliary viscosity data to get an idea of the polydispersity of the polymer. $[\eta]$ is a noninteger measure of the polymer population distribution C(M) according to

$$[\eta] = \frac{A\int M^{\alpha} C(M)\, dM}{\int C(M)\, dM} \tag{32}$$

For nonglobular polymers, α runs from 0.5 for ideal coils up to 2 for rods. For ideal random coils, $[\eta] \propto M^{0.5}$. A possible measure of polydispersity, then, is the quantity $M_w/[\eta]^2$. The related quantity M_w/η_r^2 is shown in Figure 14 for several cases and is roughly constant for reaction 3 and 4, which suggests that the polydispersity is not appreciably changing during the reaction. For reaction 7, in which M_w was deliberately changed, M_w/η_r^2 climbs markedly as the reaction proceeds, suggesting increasing polydispersity. Hence, the coupling of a viscometer with the TDSLS is a promising means of estimating polydispersity on-line, although for a given polymer a careful study would have to be done in order to relate this ratio to a readily interpretable polydispersity index.

Assessment of Random Errors. A brief consideration of the effect of random errors on the determination of M_w is now given. The effects of systematic errors due to calibration factors and dn/dc are straightforward but not pursued here.

Table 3. SD Measured on Different Detectors for Reaction 2

detector	media	σ
TDSLS	dark	0.0035 V
	water	0.0147 V
	monomer	0.0150 V
RI	monomer	9.82 10^{-6} g cm^{-3}
UV	monomer	3.00 10^{-6} g cm^{-3}

The standard deviation, or root-mean-square fluctuation, can be determined by computing it over the baseline region when pure solvent flows, before the reaction starts. The standard deviation σ_V, of any of the voltages or other quantities measured or computed follows the standard definition, as the square root of the variance, s^2, given as

$$\sigma_v = \sqrt{s_v^2} = \sqrt{\frac{1}{n-1}\sum_{i=1}^{n}(V_i - \langle V\rangle)^2} \tag{33}$$

where n is a large number of sampling points (typically 200−400 for the baselines in this work) and $\langle V\rangle$ is the average value of V over all n points.

In Table 3, values of σ_v are summarized for reaction 2 for the TDSLS, RI, and UV. As can be seen, the fluctuations of the TDSLS were smallest for the dark counts, because they were only due to electronic noise on the low-level light detector and on the A/D board. The higher standard deviations for monomer and water measured with the light scattering are due to fluctuations of the laser intensity, possibly flow effects and concentration.

Because no additional amplification was used on any of the detectors, the voltage resolution for the 12 bit A/D board with a −10 V to 10 V range was 4.9 mV. This gave a certain "graininess" to the UV signal, seen most clearly in Figure 8.

The standard deviations of the various detectors are related to root-mean-square deviations in the concentration, absolute scattered intensity, and intrinsic viscosity. For intensity,

$$\Delta I = \frac{I_{tol} F}{\langle V_{tol}\rangle}\sigma_{V,LS} \tag{34}$$

where F is defined in eq 23 above, $\langle V_{tol}\rangle$ is the net voltage of the pure toluene readings averaged over many points, and $\sigma_{V,LS}$, is the standard deviation of the light scattering detector, computed according to eq 33.

Differentiating M_w in eq 30 leads to the following relation for the mean square deviation of M_w, denoted $\Delta M_{w,i}^2$ at any point in time i,

$$\Delta M_{w,i}^2 = \left(\frac{\partial M_w}{\partial I}\right)_i^2 \langle(\Delta I)^2\rangle + \left(\frac{\partial M_w}{\partial c}\right)_i^2 \langle(\Delta c)^2\rangle + 2\left(\frac{\partial M_w}{\partial I}\frac{\partial M_w}{\partial c}\right)_i \langle \Delta I \Delta c\rangle \tag{35}$$

where the brackets denote the mean square fluctuations of the respective parameters. Because the RI and LS detectors are independent, their fluctuations are also independent, so that $\langle \Delta I \Delta c\rangle = 0$, and the fractional error

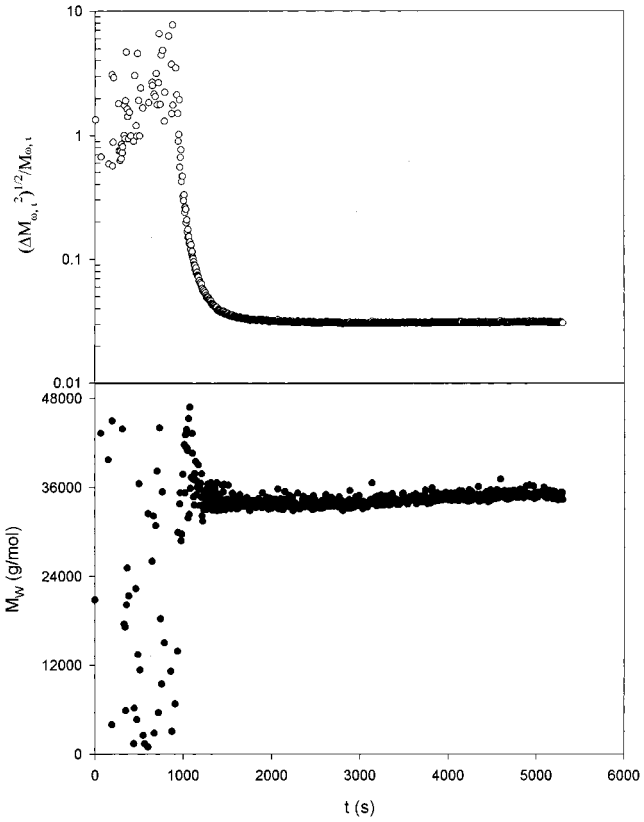

Figure 15. Fractional random error of M_w vs detector time (above) according to eq 37. Also shown below in the split graph is M_w.

in M_w, σ_{M_w}/M_w, at each sampling point can be *estimated* as

$$\left.\frac{\sigma_{M_w}}{M_w}\right|_i = \frac{\sqrt{(\Delta M_{w,i}{}^2)}}{M_{w,i}} = \frac{1}{M_{w,i}}\sqrt{\left(\left.\frac{\partial M_w}{\partial I}\right|_i\right)^2\langle(\Delta I)^2\rangle + \left(\left.\frac{\partial M_w}{\partial c}\right|_i\right)^2\langle(\Delta c)^2\rangle} \quad (36)$$

or

$$\left.\frac{\sigma_{M_w}}{M_w}\right|_i = M_{w,i}\sqrt{\left(\frac{c_i k}{I_i{}^2}\right)^2\langle(\Delta I)^2\rangle + \left(\frac{k}{I_i} - 2A_2\right)^2\langle(\Delta c)^2\rangle} \quad (37)$$

As can be seen in Figure 15, the measurement method gives reliable values after the chemical lag-time (injection of H_2O_2), which is about 1000 s for reaction 2. Afterward the random error is on the order of 3%.

Observations on the Reaction Kinetics. It is clear from the on-line results, and confirmed by the SEC, that the chains produced in the polymerization are formed very quickly and reach their approximate final value at the onset of the conversion of monomer. Hence, the initiation steps appear to be rate-limiting, whereas the propagation and termination steps are rapid compared to initiation. This is a common situation in free radical polymerization and consistent with typical lifetimes of peroxides of tens or hundreds of minutes[22] in the range of 40−80 °C. We do not have a unique explanation for the fact that M_w remains constant throughout the monomer conversion process. Another salient feature is the linear dependence of final M_w on the initial monomer to initiator concentration.

The reaction may be assumed to consist of initiation, propagation, and termination steps. We ignore chain transfer, chiefly because M_w scales linearly with monomer/initiator (Figure 6), which is not expected if chain transfer dominates.

If we ignore other possible reactions, such as first-order radical termination, the following rate equations govern the total monomer and radical concentrations, $m(t)$ and $R(t)$, respectively,

$$\frac{dm}{dt} = -2fk_i mI - k_p mR \quad (38)$$

$$\frac{dR}{dt} = 2fk_i mI - k_t R^2 \quad (39)$$

where f is the initiator efficiency, that is, the fraction of initiator that actually produces radicalized monomers. I is the concentration of free radical produced from H_2O_2 decomposition and k_i, k_p, and k_t are the initiation, propagation, and termination rate constants, respectively. These two coupled equations contains four rate constants and also the radical efficiency f. A priori, we have no guide as to the values of any of these five constants, so that we do not expect to arrive at a satisfactory description of our data with this approach here. Some comments are nonetheless in order. Often, the so-called quasi-steady-state approximation (QSSA) is invoked. This assumes that $dR/dt \sim 0$, and hence predicts that

$$R(t) = \sqrt{\frac{2fI_o k_d}{k_t}}e^{-k_d t/2} \quad (40)$$

for an initiator decomposition rate constant k_d.

The so-called "kinetic chain length" v, is the probability of a radical propagating via monomer addition divided by the probability of termination via encounter with another free radical.

$$v = \frac{k_p m}{k_t R} \quad (41)$$

In the QSSA, this is given by

$$v = \frac{k_p m}{\sqrt{2fk_d k_t I}} \quad (42)$$

This is the origin of the prediction that polymer chain length is proportional to the inverse square root of initiator concentration. Figure 6 shows that final M_w is actually inversely proportional to initiator concentration, so that the QSSA already fails at this level of prediction.

The QSSA also predicts that $m(t)$ should fall exponentially in the case of long chains and for extremely slow initiator decomposition. Figure 8 shows $m(t)$ for several of the experiments in Table 2. It is clear that none are simple exponentials. Even if the initiator decay is taken into account in the QSSA, then $m(t)$ should fall as

$$m(t) = m_o \exp\left[\left(\frac{8fk_p{}^2 I_o}{k_t k_d}\right)^{1/2}(e^{-k_d t} - 1)\right] \quad (43)$$

The curves of $m(t)$ in Figure 8, however, do not conform to this function, nor to any other simple function which could result from simple approximations to the rate equations. Furthermore, inspection of eq 43 shows that it can lead to a dead-end polymerization, in which not all monomer is consumed. The UV data indicate, however, that all the VP monomer is consumed to within the detection limit of the UV monitor, except in experiment 8, where a deliberate attempt at dead-end polymerization was made.

The existence of the M_w plateau for most reactions, however, still suggests some sort of steady-state. If the notion of kinetic chain length is valid, i.e., that the instantaneous degree of polymerization is proportional to $m(t)/R(t)$, then a constant M_w implies this ratio is constant,

$$\frac{m(t)}{R(t)} \approx \frac{m_o}{R_o} \tag{44}$$

i.e., the monomer and radical concentrations decrease at the same rate (here m_o and R_o refer to the monomer and initiator concentrations, respectively, when the M_w plateau begins). A kinetic model for this condition must hence be found. A purely mathematical condition can be found as follows. The rate equations lead to

$$\frac{dm}{dR} = \frac{-k_p m R}{2fk_d m I - k_t R^2} \tag{45}$$

where the experimentally justified long chain approximation is used that $2fk_dI \ll k_p mR$; i.e., most monomer is lost being incorporated in chains and not merely in being radicalized. If, additionally, $2fk_dI \ll k_tR^2$, then it follows that

$$\frac{m(t)}{m_o} = \left(\frac{R(t)}{R_o}\right)^{k_p/k_t} \tag{46}$$

In this case $m(t)/R(t)$ can only be constant if $k_p = k_t$ on the plateau. This may not seem unreasonable, as it implies that upon encounter, a radical is as likely to react with a monomer as with another radical. In light of many literature reports, however, it seems unlikely that k_p is really equal to k_t. Odian[13] reports, for example, that k_t is usually about 4 orders of magnitude greater than k_p ($k_t \approx 10^6-10^8$ and $k_t \times 10^2-10^4$). Kaplan and Rodriques[9] measured the rate constants for VP polymerization with a rotating sector experiment using azobisdiisobutyronitrile. They found at 30 °C, when retardation effects were absent, that $k_t \times 2.59 \times 10^7$ mol s^{-1} L^{-1} and $k_p \times 1.25 \times 10^3$ mol s^{-1} L^{-1}. Hence there is reason to believe there is a more physically suitable explanation for constant M_w than the mathematical explanation leading to $k_p = k_t$.

"Retardation" effects may also be seen throughout the data in this work, even after corrections for lag-times are made (Figures 1−5, 8−10). Figure 8 shows that the initial plateau of $m(t)$ gets longer as the ratio of monomer to initiator increases at fixed T. This initial plateau, or region of slow decrease, can be approximated from eqs 38 and 39 for early t. Considering $I(t) = I_o$ at the outset and initiator dissociation and monomer radicalization as lumped together allows immediate

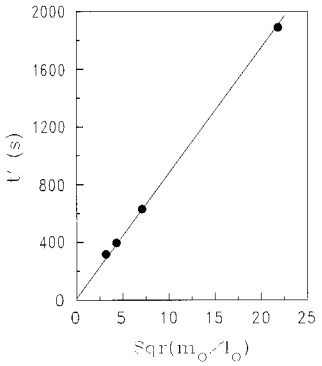

Figure 16. The time it takes for $m(t)$ to fall to $0.9m_o$, t′, vs the reciprocal square root of initial initiator concentration. The linear result indicates that the "chemical lag-time" is a natural consequence of the onset of polymerization, contained in eq 47, valid at early times.

solution of eq 39 and integration of eq 38 to yield a solution for $m(t)$ of

$$m(t) = m_o\,(\cosh(t\sqrt{2fk_dk_tI_o}))^{-k_p/k_t} \tag{47}$$

This function qualitatively conforms to the initial behavior of $m(t)$ in the different curves of Figure 8. Decreasing I_o stretches out the initial plateau, consistent with the experiments. Decreasing the ratio k_p/k_t would also stretch out the plateau. Referring to $m(t)$ data, such as in Figure 8, a value of $m(t)/m_o = 0.9$ was chosen, and the time t′ at which this value occurred is plotted vs $(m_o/I_o)^{1/2}$ in Figure 16. The result is quite linear, as inversion of eq 47 requires:

$$t' = \frac{\cosh^{-1}[(1.11)^{k_t/k_p}]}{\sqrt{2fk_dk_tI_o}} \tag{48}$$

Hence, the "chemical lag-time" in the various experiments is simply due to the predicted hyperbolic cosine form of $m(t)$ resulting from the solution to eqs 38 and 39 at early times.

Inhibition (or retardation) caused by impurities, such as oxygen in the monomer or solvent, can also have a considerable effect on radical polymerizations. The repeatability of the experiments and the close linear relationship of final M_w on initial monomer to initiator concentration, however, suggest that effects due to impurities, poor degassing, etc., are probably quite negligible.

In many situations the diffusion-controlled rate constants can change as polymerization proceeds. Diffusion effects are often separated into three phenomena:[7] the gel, the glass, and the cage effects. The latter takes into account the possibility of recombination of primary radicals, which may be very soon after their generation. The cage effect is normally corrected for by the efficiency f. However, f could change during the reaction due to viscosity increase. The decrease of the mobility of monomer is described by the glass effect, which results in a decrease of k_p. A decrease of the termination rate k_t (the gel effect) is caused by a decrease of the mobility of the polymer chains and leads to an increase in M_w. This effect was originally discussed by Trommsdorf.[15] Given the constancy of the M_w plateau for the low final M_w experiments, it seems that diffusion effects may be completely absent in those data. For the higher final M_w, such as experiment 4, there is a measurable

increase of M_w after a high M_w is reached, which may be associated with a viscosity effect such as that described by Trommsdorf. One might think that the polydispersity should be higher for experiment 4 than the others. Within error bars, however, it is similar to the other experiments. This may be due to the fact that, although increasing, M_w increases over a fairly narrow range of ~60−100K (a 20% variation over the mean) during the reaction, whereas the polydispersity value shows that M_z is 250% greater than M_w, so the narrow variation is "buried" in the large width of the distribution.

Summary

Coupled TDSLS, RI, UV absorbance, and viscosity detectors have been used to demonstrate the acquisition of $M_w(t)$, $C_p(t)$, m(t), and $\eta_r(t)$ on-line. The advantages of this for developing new polymers and carrying out quality control of large-scale industrial reactors are clear. It is important that the reacting solution be diluted to a concentration such that the light scattering intensity is controlled by $M_w(t)$ and not the concentration-dependent virial coefficient terms.

The curves generated conformed to the general expectations that increasing monomer to initiator concentration should lead to higher masses and that higher monomer concentration should lead to faster reactions. As expected, higher temperature led to faster reactions and smaller M_w. The data show that chains are produced very quickly and yield a value of M_w that remains remarkably constant throughout the rest of the reaction. SEC on periodically withdrawn aliquots from one experiment confirmed this on-line result and also showed that the polydispersity M_z/M_w quickly climbed to a plateau value of about 2.5. Finally, by injecting additional initiator into a reaction in progress, it was demonstrated that the ensuing changes in M_w could be followed.

Acknowledgment. The authors gratefully acknowledge the Louisiana Board of Regents University/Industry ties grant RD-B-11 and the Center for Photoinduced Processes funded by the National Science Foundation and the Louisiana Board of Regents. F.H.F. acknowledges support from Brazil's CNPq. We thank Edson Minatti for introducing us to the procedures involved in the PVP reaction.

References and Notes

(1) Reed, W. F. *J. Chem. Phys.* **1995**, *103*, 7576−7584.
(2) Catalani, L. H.; Rabello, A. M.; Florenzano, F. H.; Politi, M. J.; Reed, W. F. *Int. J. Polym. Anal. Charact.* **1997**, *3*, 231−247.
(3) Reed, C. E.; Reed, W. F. *J. Chem. Phys.* **1989**, *91*, 7193−7199.
(4) Ghosh, S.; Reed, W. F. *Biopolymers* **1995**, *35*, 435−450.
(5) Reed W. F. *Macromol. Chem. Phys.* **1995**, *196*, 1539−1575.
(6) Reed W. F., *Strategies in Size Exclusion Chromatograpy*; ACS symposium series 635; Potschka, M., Dubin, P., Eds.; American Chemical Society: Washington DC, 1996; pp 7−34.
(7) Achillas, D. S.; Kipparissides, C. *Macromolecules* **1992**, *25*, 3739−3750.
(8) Stevenson, J. F. *Polym. Eng. Sci.* **1986**, *26*, 746−759.
(9) Kaplan, R. H.; Rodriquez, F. *Appl. Polymer Symp.* **1975**, *26*, 181−195.
(10) Gaylord, N. G. *Appl. Polymer Symp.* **1975**, *26*, 197−209.
(11) Senogles, E.; Thomas, R. *J. Polymer Sci.* **1975**, *49*, 203-210.
(12) Boyd, R. H.; Phillips, P. J. *The Science of Polymer Molecules*; Cambridge University Press: Cambridge, 1996.
(13) Odian, G. *Principles of Polymerization*; John Wiley & Sons: New York, 1991.
(14) Dotson, N. A.; Galvan, R.; Laurence, R. L.; Tirrel, M. *Polymerization Process Modelling*; VCH Pub.: New York, 1996.
(15) Trommsdorf, E.; Kohle, H.; Lagally, P. *Makromol. Chem.* **1948**, *1*, 169−177.
(16) Zimm, B. H. *J. Chem. Phys.* **1948**, *16*, 1093−1099.
(17) Fikentscher, H. F.; Herrle, K. *Mod. Plast.* **1945**, *23*, 157−198.
(18) Norwood, D. P.; Reed, W. F. *Int. J. Polym. Anal. Charact.* **1997**, *4*, 99−132.
(19) Bender, T. M.; Lewis, R.; Pecora, R. *Macromolecules* **1986**, *19*, 244−247.
(20) Benoit, H.; Benmouma, M. *Polymer* **1984**, *52*, 1059−1072.
(21) Stockmayer, W. H. *J. Chem. Phys.* **1950**, *18*, 50−67.
(22) Clayton, W. *Trans. Faraday Soc.* **1915**, *2*, 164−171.

MA980876E